PAPER • OPEN ACCESS

Neutron star structure with chiral interactions

View the article online for updates and enhancements.

Neutron star structure with chiral interactions

Domenico Logoteta[1] **and Ignazio Bombaci**[2]

[1]INFN, Sezione di Pisa, Largo Bruno Pontecorvo 3, I-56127 Pisa, Italy

[2]Dipartimento di Fisica, Universitá di Pisa, Largo Bruno Pontecorvo 3, I-56127 Pisa, Italy and INFN, Sezione di Pisa, Largo Bruno Pontecorvo 3, I-56127 Pisa, Italy

E-mail: [1]domenico.logoteta@pi.infn.it

E-mail: [2]ignazio.bombaci@unipi.it

Abstract. We use two-body and three-body nuclear interactions derived in the framework of chiral perturbation theory (ChPT) with and without the explicit Δ isobar contributions to calculate the energy per particle of symmetric nuclear matter and pure neutron matter employing the microscopic Brueckner–Hartree–Fock approach. In particular, we present nuclear matter calculations using the new fully local in coordinate-space two-nucleon interaction at the next-to-next-to-next-to-leading-order (N3LO) of ChPT with Δ isobar intermediate states (N3LOΔ) recently developed by Piarulli *et al.* [1]. We compute the β-equilibrium equation of state and determine the neutron star mass-radius and mass-central density sequences. We find that the adopted interactions are able to provide satisfactory properties of nuclear matter at saturation density as well as to fulfill the limit of two-solar mass for the maximum mass configuration as required by recent observations.

1. Introduction

Chiral effective field theory (EFT) opened a new avenue for a description of nuclear interactions [2, 3, 4]) and nuclear systems consistent with quantum chromodynamics (QCD), the fundamental theory of the strong interaction. The considerable advantage of using such method lies in the fact that two-body, three-body as well as many-body nuclear interactions can be calculated perturbatively, i.e. order by order, according to a well defined scheme based on a low-energy effective QCD Lagrangian which retains the symmetries of QCD, and in particular the approximate chiral symmetry. Within this chiral perturbation theory (ChPT) the details of the QCD dynamics are contained in parameters, the so called low-energy constants (LECs), which are fixed by low-energy experimental data.

Recently Piarulli et al. [1] have developed a fully local in coordinate-space two-nucleon chiral potential which includes the Δ isobar intermediate state. This new potential represents the fully local version of the minimally non-local chiral interaction reported in Ref. [5]. It has been shown by various authors [6, 7] that a Δ-full ChPT has an improved convergence with respect to the Δ-less ChPT. In addition, the Δ-full ChPT naturally leads to three-nucleon forces (TNFs) induced by two-pion exchange with excitation of an intermediate Δ (the celebrated Fujita–Miyazawa three-nucleon force [8]).

In this work, we present microscopic calculations of the equation of state (EoS) of symmetric nuclear matter and pure neutron matter using the local chiral potential of Ref. [1] and employing the Brueckner–Bethe–Goldstone (BBG) [9, 10] many body theory within the Brueckner–Hartree–Fock (BHF) approximation. The present work contains some of the results published in

Ref. [11] and represents a development with respect to our previous works [12, 13] where ChPT nuclear interactions have been used in BHF calculations of nuclear matter properties.

2. Chiral nuclear interactions

Let us now focus on the specific interactions we have employed in the present work. Among the large variety of nucleon-nucleon (NN) interactions derived in the framework of ChPT, as the two-body nuclear interaction, we have used the fully local chiral potential at N3LO including Δ isobar excitations in intermediate state (hereafter N3LOΔ) recently proposed in Ref. [1]. Originally this potential was presented in Ref. [5] in a minimal non-local form. Notice that Ref. [1] reports different parametrizations of the local potential obtained by fitting the low energy NN experimental data using different long- and short-range cutoffs. In the calculations presented in this work, we use the *model b* described in Ref. [1] (see their Tab. II) which fits the Granada database [14] of proton-proton (pp) and neutron-proton (np) scattering data up to an energy of 125 MeV in the laboratory reference frame and has a $\chi^2/\text{datum} \sim 1.07$.

To compare with other NN interactions, we have also employed the N3LO chiral NN potential by Entem and Machleidt (EM) [15], considering two different values of the cutoff, $\Lambda = 500$ MeV and $\Lambda = 450$ MeV, employed to regularize the high momentum components of the interaction. Notice that for consistency reasons, the same value of the cutoff has been employed in each calculation, both in the two- and three-nucleon interactions. However the assumed shape of the cutoff in the two-body and in the three-body interaction is in general different (see Ref. [11] for more details).

Concerning the TNF, we have used the N2LO potential by Epelbaum et al. [16] in its local version given by Navratil [17]. We note that the non locality of the N2LO three-nucleon interaction depends only on the cutoff used to regularize the potential. The N2LO TNF depends on factors c_1, c_3, c_4, c_D and c_E which are the so called low energy constants. The N2LO interaction keeps the same operatorial structure both including or not the Δ degrees of freedom ([7]). We note that the constants c_1, c_3 and c_4 are already fixed at the two-body level by the N3LO interaction. However when including the Δ isobar in the three-body potential, the parameters c_3 and c_4 take additional contribution from the Fujita–Miyazawa diagram. Such a diagram appears at the NLO and is clearly not present in the theory without the Δ (see discussion in Ref. [11] about this issue). The values of the constants c_i for the TNFs that we have considered in the present work are reported in Tab. 1.

The remaining parameters c_D and c_E are not determined by the two-body interaction and have to be fixed constraining some specific observables in few-nucleon systems or to reproduce the empirical saturation point of symmetric nuclear matter. In particular, for the interaction model N3LO+N2LO(450), following reference [18], we have set $c_D = -0.24$ and $c_E = -0.11$ in order to reproduce the binding energies of ^{3}H and ^{3}He and the Gammow-Teller matrix element for the ^{3}H β-decay considering contributions to the axial nuclear current up to order N3LO [18]. For the interaction model N3LO+N2LO(500), we have adopted a recent constraint on c_D and c_E employing the same strategy of Ref. [18] but considering contributions to the axial nuclear current up to order N4LO [19]. We note that this parametrization has also the valuable property to reproduce the neutron–deuteron doublet scattering length.

Finally, for the very recent model N3LOΔ+N2LOΔ [1] no calculation for few-body nuclear systems has been done so far. Thus we have fitted the LECs c_D and c_E to get a good saturation point for symmetric nuclear matter.

3. The Brueckner–Hartree–Fock approach with averaged three-body forces

The BHF approach is the lowest order of the BBG many-body theory [9, 10]. In this theory, the ground state energy of nuclear matter is evaluated in terms of the so-called hole-line expansion, where the perturbative diagrams are grouped according to the number of independent hole-lines.

Table 1. Values of the low energy constants (LECs) of the TNFs models used in the present calculations. In the first row, we report the parametrizations of the N2LO three-body force with the Δ isobar excitations [1]. Notice that the values c_1, c_3 and c_4 have been kept fixed. In the third and in the forth rows we report the N2LO TNF parametrizations obtained in conjunction with the EM [15] N3LO two-nucleon potential with $\Lambda = 500$ MeV (third row) and with $\Lambda = 450$ MeV (forth row). The LECs c_1, c_3 and c_4 are expressed in GeV^{-1}, whereas c_D and c_E are dimensionless.

TNF	c_D	c_E	c_1	c_3	c_4
N2LOΔ	-0.10	1.30	-0.057	-3.63	3.14
N2LO500	-1.88	-0.48	-0.810	-3.20	5.40
N2LO450	-0.11	-0.24	-0.810	-3.40	3.40

The expansion is derived by means of the in-medium two-body scattering Brueckner G-matrix which describes the effective interaction between two nucleons in presence of the surrounding nuclear medium. In the case of asymmetric nuclear matter [1] with neutron density ρ_n, proton density ρ_p, total nucleon density $\rho = \rho_n + \rho_p$ and isospin asymmetry $\beta = (\rho_n - \rho_p)/\rho$ (asymmetry parameter), one has different G-matrices describing the nn, pp and np in medium effective interactions. They are obtained by solving the well known Bethe–Goldstone equation [9].

We make use of the so-called continuous choice [22] for the single-particle potential $U_\tau(k)$ when solving the Bethe–Goldstone equation. As shown in Refs. [23, 24], the contribution of the three-hole-line diagrams to the energy per particle E/A is minimized in this prescription and a faster convergence of the hole-line expansion for E/A is achieved [23, 24, 25] with respect to the so-called gap choice for $U_\tau(k)$.

As it is well known, within the most advanced non-relativistic quantum many-body approaches [26], it is not possible to reproduce the empirical saturation point of symmetric nuclear matter, $\rho_0 = 0.16 \pm 0.01$ fm^{-3}, $E/A|_{\rho_0} = -16.0 \pm 1.0$ MeV, when using two-body nuclear interactions only. In addition, TNFs are crucial in the case of dense β-stable nuclear matter to obtain a stiff equation of state (EoS) [27, 28] compatible with the measured masses, $M = 1.97 \pm 0.04\,M_\odot$ [29] and $M = 2.01 \pm 0.04\,M_\odot$ [30] of the neutron stars in PSR J1614-2230 and PSR J0348+0432 respectively.

Within the BHF approach TNFs cannot be used directly in their original form. This is because it would be necessary to solve the three-body Faddeev equations in the nuclear medium (Bethe–Faddeev equations) [31, 32] and currently this is a task still far to be achieved. To circumvent this problem an effective density dependent two-body force is built starting from the original three-body one by averaging over one of the three nucleons [33, 34].

In the present work, we consider the in medium effective NN force derived in Ref. [35] (see Ref. [11] for more details on the average).

4. Results and discussion
In this section we present and discuss the results of our calculations for the equation of state (EoS), i.e. the energy per particle E/A as a function of the density ρ, for symmetric nuclear matter (SNM) and pure neutron matter (PNM) using the chiral nuclear interaction models and the BHF approach described in the previous two sections. In all the calculations performed

---

[1] In the present work we consider spin unpolarized nuclear matter. Spin polarized nuclear matter within the BHF approach has been considered, for example, in Ref. [20, 21].

Table 2. Nuclear matter properties at saturation point for the models described in the text. In the first column we report the model name; in the other columns we give the saturation density (ρ_0) of symmetric nuclear matter, the corresponding value of the energy per particle E/A, the symmetry energy, its slope parameter L and the incompressibility K_∞. All these values refer to the calculated saturation density.

Model	$\rho_0(\text{fm}^{-3})$	E/A (MeV)	E_{sym} (MeV)	L (MeV)	K_∞ (MeV)
N3LOΔ+N2LOΔ	0.171	-15.23	35.39	76.0	190
N3LO+N2LO(500)	0.135	-12.12	25.89	38.3	153
N3LO+N2LO(450)	0.156	-14.32	29.20	39.8	205

in this work, we have considered partial wave contributions up to a total two-body angular momentum $J_{max} = 8$.

In Fig. 1 we show the energy per particle of PNM [panel (a)] and SNM [panel (b)] for the considered interaction models. The dashed lines, in both panels, refer to the calculations performed employing the two-body potential without any TNF, whereas the continuous lines refer to the calculations where the contribution of the TNFs to the energy per nucleon has been included.

Focusing first on the case of PNM (Fig. 1(a)), we note sizable differences between the three energy per nucleon curves produced by the different NN interactions. The model N3LOΔ (upper (black) dashed line) gives indeed a much stiffer EoS than the N3LO ones for both cutoff values, $\Lambda = 500$ MeV (middle (red) dashed line) and $\Lambda = 450$ MeV (lower (blue) dashed line). This behaviour is both due to the local form of the potential and to the inclusion of Δ isobar.

In addition, looking at Tab. 1, we see that the values of c_1 and c_3 are very similar for the considered models. Thus we expect a comparable effect of TNFs on the EoS for PNM as confirmed by our results.

The EoS for symmetric nuclear matter is shown in Fig. 1(b). When only two-body interactions are included, the models based on the EM N3LO potential [15] give unsatisfactory nuclear matter saturation properties. More specifically the model N3LO(500) (middle (red) dashed line) gives a saturation point ($\rho_0 = 0.41$ fm^{-3}, $E/A|_{\rho_0} = -24.25$ MeV), whereas the EoS curve for the model N3LO(450) (lower (blue) dashed line) shows no saturation point up to density of ~ 0.5 fm^{-3}. The EoS for the N3LOΔ NN interaction [1] (upper (black) dashed line) has instead a very different trend. In this case the saturation point turns out to be (0.24 fm^{-3}, -18.27 MeV).

The overall repulsive effect introduced by the inclusion of TNFs produces a significant improvement of the calculated SNM saturation point (see the continuous lines in Fig. 1(b)) with respect to the results described above for the case with no TNFs.

These results clearly show that in the case of Δ-full chiral nuclear interactions the contribution to the energy per particle generated by the TNFs is strongly reduced in comparison to the case where the EoS is obtained from Δ-less chiral interactions.

In Tab. 2 we report the calculated values of the saturation points of SNM for the interaction models considered in the present work. All the models, with the exception of the N3LO+N2LO(500) one, provide reasonable saturation points.

The energy per nucleon of asymmetric nuclear matter can be accurately reproduced [36] using the so called parabolic (in the asymmetry parameter β) approximation

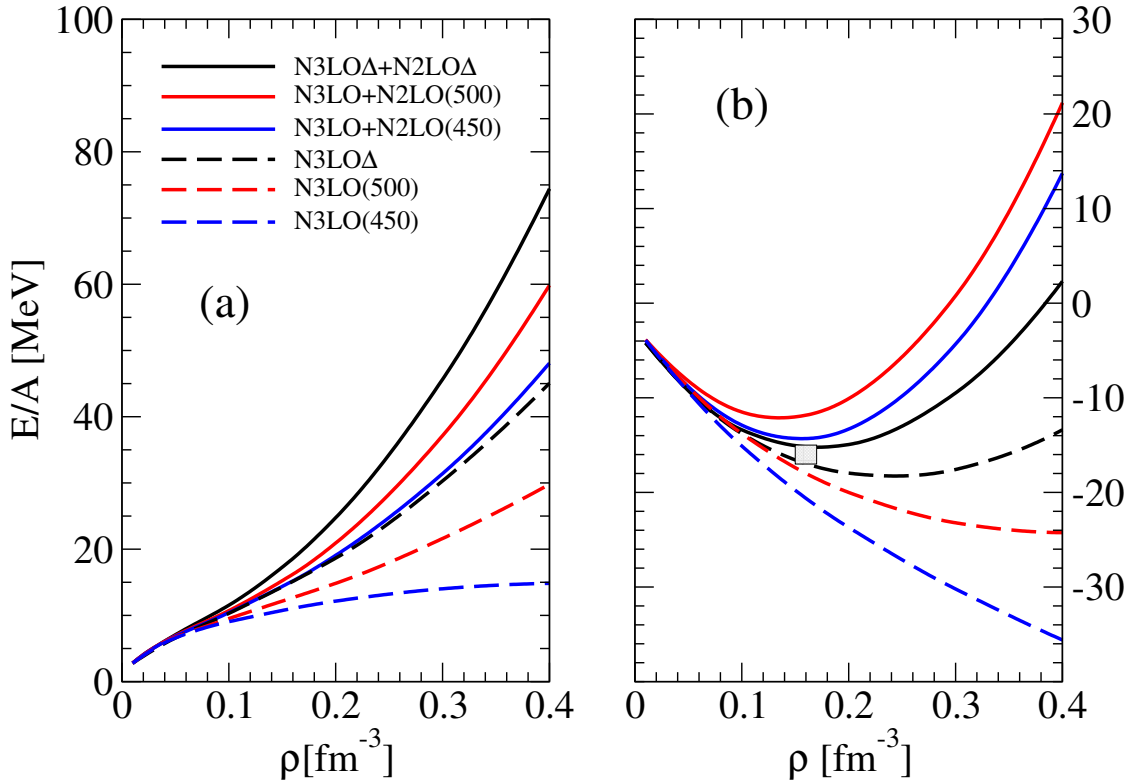$$\frac{E}{A}(\rho, \beta) = \frac{E}{A}(\rho, 0) + E_{sym}(\rho)\beta^2 \, . \tag{1}$$

Figure 1. (Color online) Energy per particle of pure neutron matter [panel (a)] and symmetric nuclear matter [panel (b)] as a function of the nucleonic density for the models described in the text. Continuous lines have been obtained using two- plus three-body interactions, while the dashed lines have been obtained considering only the two-body interaction. The empirical saturation point of nuclear matter $\rho_0 = 0.16 \pm 0.01$ fm^{-3}, $E/A|_{\rho_0} = -16.0 \pm 1.0$ MeV is denoted by the grey box in the panel (b).

where $E_{sym}(\rho)$ is the nuclear symmetry energy [37]. Using Eq. (1), the symmetry energy can be calculated as the difference between the energy per particle of pure neutron matter ($\beta = 1$) and symmetric nuclear matter ($\beta = 0$).

In Tab. 2 we report the symmetry energy and the so called slope parameter

$$L = 3\rho_0 \frac{\partial E_{sym}(\rho)}{\partial \rho}\bigg|_{\rho_0} \tag{2}$$

at the calculated saturation density ρ_0 (second column in Tab. 2) for the interaction models considered in the present work. As we can see our calculated $E_{sym}(\rho_0)$ and L are in a satisfactory agreement with the values obtained by other BHF calculations with two- and three-body interactions (see e.g. [38, 39]) and with the values extracted from various experimental data, $E_{sym}(\rho_0) = 29.0 - 32.7$ MeV, and $L = 40.5 - 61.9$ MeV, as summarized in Ref. [40].

The incompressibility K_∞ of symmetric nuclear matter at saturation density is given by:

$$K_\infty = 9\rho_0^2 \frac{\partial^2 E/A}{\partial \rho^2}\bigg|_{\rho_0} . \tag{3}$$

The incompressibility K_∞ is usually extracted from experimental data of giant monopole resonance (GMR) energies in medium-mass and heavy nuclei. This analysis gives $K_\infty = 210 \pm 30$

MeV [41] or more recently $K_\infty = 240 \pm 20$ MeV [42]. Recently the authors of Ref. [43] performed a re-analysis of GMR data finding 250 MeV$< K_\infty <$ 315 MeV. The incompressibility K_∞, at the calculated saturation point for the various interaction models used in the present work, is reported in the last column of Tab. 2. These calculated values for K_∞ are rather low when compared with the empirical values extracted from GMR in nuclei. This is a common feature with many other BHF nuclear matter calculations with two- and three-body interactions (see e.g. [39].

5. Neutron star structure

The composition of the inner core of a neutron star cannot be completely constrained by observations and thus different possibilities are currently under investigation. The appearence of hyperons ([44]) and the transition to a deconfined quark phase ([45, 46, 47, 48]) are among the most popular possibilities. In this work we consider the simplest case of nucleonic matter. Our aim is to establish if nuclear matter EoSs derived from modern chiral interactions can fulfill the constraints put by astrophysical observations. This is an essential step in order to consider more sophisticated possibilities. We thus apply our new EoS model based on the N3LOΔ+N2LOΔ chiral interaction to determine the structure of neutron stars [49]. To this end we calculate the EoS for β-stable nuclear matter including the lepton contribution. The composition of β-stable matter is fixed by the relations between the chemical potentials of the various species. As we are considering pure nucleonic neutrino-free matter one has:

$$\mu_n - \mu_p = \mu_e \ , \qquad \mu_e = \mu_\mu. \tag{4}$$

In Eq. (4) μ_n, μ_p, μ_e and μ_μ are the chemical potentials of neutrons, protons, electrons and muons (with muons appearing above a threshold density given by $\mu_e = m_\mu$) Finally charge neutrality requires:

$$\rho_p = \rho_e + \rho_\mu \tag{5}$$

The various chemical potentials are determined through:

$$\mu_N = \frac{\partial \epsilon}{\partial \rho_N} \ , \qquad \mu_l = \frac{\partial \epsilon}{\partial \rho_l} \tag{6}$$

where $\epsilon = \epsilon_{NN} + \epsilon_L$ is the total energy density which sums up the lepton contribution ϵ_L and the nucleonic one ϵ_{NN}.

The last one is calculated in BHF approximation from $\epsilon_{NN} = \rho \, E/A(\rho, \beta)$ where we have used the parabolic approximation to determine $E/A(\rho, \beta)$ for asymmetric matter. We have self consistently solved the equations (4), (5), (6) and obtained the EoS for $\beta-$stable matter.

Next to calculate the structure of neutron stars, we have integrated the hydrostatic equilibrium equations in general relativity [49]. For nucleonic density ≤ 0.08 fm^{-3} we have matched our EoS (which describe the neutron star core) with the Baym–Pethick–Sutherland [50] and Negele–Vautherin [51] EoS for the stellar crust. The results are shown in Fig. 2 where we plot the mass-radius (left panel) and mass-central density (right panel) relations for the considered EoS model. The hatched region in the left panel of Fig. 2 represents the mass-radius constraints based on the analysis of recent observations of both transient and bursting X-ray sources obtained in [52, 53].

The maximum mass predicted by our model, $M_{max} = 2.07 \, M_\odot$, is compatible with the accurate measurement of the masses, $M = 1.97 \pm 0.04 \, M_\odot$ [29] and $M = 2.01 \pm 0.04 \, M_\odot$ [30], of the neutron stars in PSR J1614-2230 and PSR J0348+0432 respectively. In addition our EoS model is also able to fulfill the empirical constraints on mass-radius relationship obtained in Refs. [52, 53].
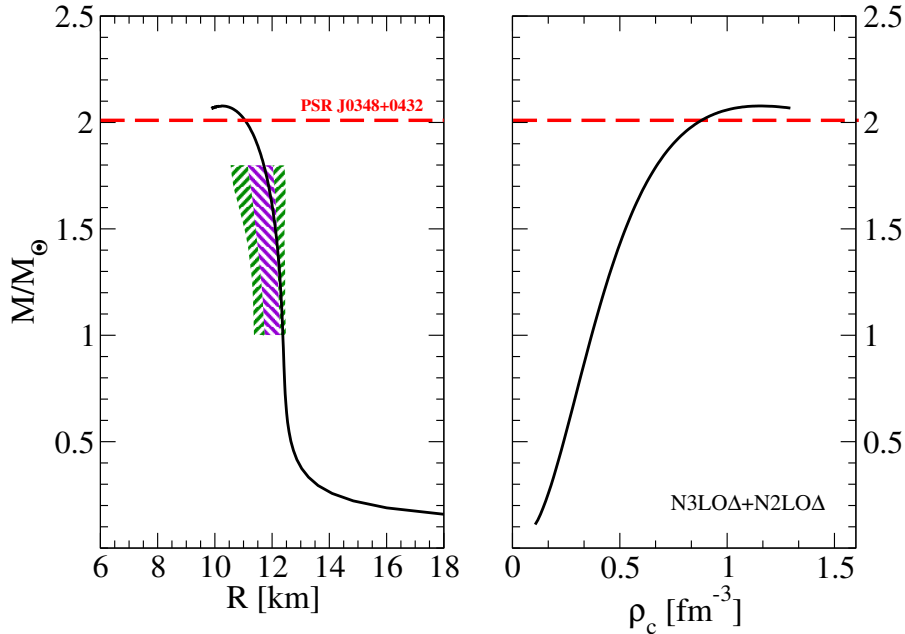
Figure 2. Mass-radius relationship (left panel) and mass-central density relationship (right panel) for the N3LOΔ+N2LOΔ model. The hatched region in the left panel represents the mass-radius constraints obtained in [52, 53]. The red dashed line stands for the measured mass of PSR J0348+0432 [30]. $M_\odot = 1.9885 \times 10^{33}$ g is the mass of the sun.

The values for the gravitational maximum mass M_{max} and the correspondig radius R and central density ρ_c are reported in Tab. 3 and are in good agreement with the results of other calculations [27, 28] based on microscopic approaches.

Table 3. Properties of the maximum mass configuration for the N3LOΔ+N2LOΔ EoS model.

Model	M_{max} ($M_\odot$)	R (km)	ρ_c (fm^{-3})
N3LOΔ+N2LOΔ	2.07	10.26	1.15

6. Summary

We have investigated the behavior and the properties of nuclear matter using three microscopic models fully based on interactions derived in chiral effective field theory, in the framework of the Brueckner–Hartree–Fock many-body approach. In particular we have tested, the new fully local chiral potential at order N3LO which includes the Δ isobar contributions in the intermediate states of the NN interaction [1]. We have also considered two versions of the N3LO chiral NN potential by Entem and Machleidt [15], which differ in the value of the cutoff employed in the calculations. All the two-nucleon interactions have been supplemented with TNFs required to satisfactorily reproduce the empirical saturation point of symmetric nuclear matter. Our results for various nuclear matter properties at saturation density are in good agreement with the available experimental data except for the incompressibility K_∞ which is underestimated with respect to the highly uncertain empirical value [41, 42, 43].

Finally for the N3LOΔ+N2LOΔ chiral interaction, we have calculated the EoS of β-stable nuclear matter and the corresponding neutron star properties. We have found that the maximum mass obtained with our EoS model is compatible with present measured neutron star masses. In addition, our calculated neutron star masses and radii are in good agreement with the empirical constraints on these quantities based on the analysis of recent observations of both transient and bursting X-ray sources obtained in [52, 53].

Acknowledgments

References

[1] Piarulli M, Girlanda L, Schiavilla R, Kievsky A, Lovato A, Marcucci L E, Pieper S C, Viviani M and Wiringa R B 2016 Phys. Rev. C **94** 054007
[2] Weinberg S 1979 Physica A **96** 327; 1990 Phys. Lett. B **251** 288; 1991 Nucl. Phys. B **363** 3; 1992 Phys. Lett. B **259** 114
[3] Epelbaum E, Hammer H-W and Meißner U G 2009 Rev. Mod. Phys. **81** 1773
[4] Machleidt R and Entem D R 2011 Phys. Rep. **503** 1
[5] Piarulli M, Girlanda L, Schiavilla R, Navarro Perez R, Amaro J E and Ruiz Arriola E 2015 Phys. Rev. C **91** 024003
[6] Kaiser N, Gerstendörfer S and Weise W 1998 Nucl. Phys. A **637** 395
[7] Krebs H, Epelbaum E and Meißner U G 2007 Eur. Phys. J. A **32** 127
[8] Fujita J and Miyazawa H 1957 Prog. Theor, Phys. **17** 360
[9] Day B D 1967 Rev. Mod. Phys. **39** 719
[10] Baldo M and Burgio G F 2012 Rep. Progr. Phys. **75** 026301
[11] Logoteta D, Bombaci I and Kievsky A 2016 Phys. Rev. C **94** 064001
[12] Logoteta D, Vidaña I, Bombaci I and Kievsky A 2015 Phys. Rev. C **91** 064001
[13] Logoteta D, Bombaci I and Kievsky A 2016 Phys. Lett. B **758** 449
[14] Navarro Pérez R, Amaro J E and Ruiz Arriola E 2013 Phys. Rev. C **88** 064002; Erratum 2015 Phys. Rev. C 91 029901
[15] Entem D R and Machleidt R 2003 Phys. Rev. C **68** 041001(R)
[16] Epelbaum E, Nogga A, Glöckle W, Kamada H and Meißner U G and Witała H 2002 Phys. Rev. C **66** 064001
[17] Navratil P 2007 Few-Body Syst. **41** 117
[18] Marcucci L E, Kievsky A, Rosati S, Schiavilla R and Viviani M 2012 Phys. Rev. Lett. **108** 052502
[19] Baroni A, Girlanda L, Kievsky A, Marcucci L E and Viviani M 2016 Phys. Rev. C **94** 024003.
[20] Vidaña I and Bombaci I 2002 Phys. Rev. C **66** 045801
[21] Bombaci I, Polls A, Ramos A, Rios A and Vidaña I 2006 Phys. Lett. B **632** 638
[22] Jeukenne J P, Lejeunne A and Mahaux C 1976 Phys. Rep. **25** 83
[23] Song H Q, Baldo M, Giansiracusa G and Lombardo U 1998 Phys. Rev. Lett. **81** 1584
[24] Baldo M, Giansiracusa G, Lombardo U and Song H Q 2000 Phys. Lett. B **473** 1
[25] Baldo M, Bombaci I, Giansiracusa G and Lombardo U 1990 J. Phys. G: Nucl. Part. Phys. **16** L263
[26] Bombaci I, Fabrocini A, Polls A and Vidaña I 2005 Phys. Lett. B **609** 232
[27] Baldo M, Bombaci I and Burgio G F 1997 Astron. and Astrophys. **328** 274
[28] Akmal A, Pandharipande V R and Ravenhall D G 1998 Phys. Rev. C **58** 1804
[29] Demorest P, Pennucci T, Ransom S, Roberts M and Hessels J 2010 Nature **467** 1081
[30] Antoniadis J et al. 2013 Science **340** 1233232
[31] Bethe H A 1965 Phys. Rev. **138** 804B
[32] Rajaraman R and Bethe H A 1967 Rev. Mod. Phys. **39** 745
[33] Loiseau B A, Nogami Y and Ross C K 1971 Nucl. Phys. **A401** 601
[34] Grangé P, Lejeunne A, Martzolff B and Mathiot J-F 1989 Phys. Rev.C **40** 1040
[35] Holt J W, Kaiser N and Weise W 2010 Phys. Rev. C **81** 024002
[36] Bombaci I and Lombardo U 1991 Phys. Rev. C **44** 1892
[37] Eur. Phys. J. A **50** (2) 2014, Topical issue on Nuclear Symmetry Energy, edited by Li B A, Ramos A, Verde G and Vidaña I
[38] Li Z H, Lombardo U, Schulze H-J, Zuo W, Chen L W and Ma H R 2006 Phys. Rev. C **74** 047304
[39] Li Z H and Schulze H-J 2008 Phys. Rev. C **78** 028801
[40] Lattimer J M 2014 Gen. Rel. Grav. **46** 1713

[41] Blaizot J P, Gogny D and Grammaticos B 1976 Nucl. Phys. A **265** 315
[42] Sholmo S, Kolomietz V K and Colò G 2006 Eur. Phys. J. A **30** 23
[43] Stone J R, Stone N J and Moszkowski S A 2014 Phys. Rev. C **89** 044316
[44] Vidaña I, Logoteta D, Providência C, Polls A and Bombaci I 2011 EPL **94** 11002
[45] Bombaci I, Logoteta D, Vidaña I and Providência C 2016 EPJA **52** 58
[46] Logoteta D, Bombaci I, Providência C and Vidaña I 2012 Phys. Rev. C **85** 055807
[47] Logoteta D, Providência C and Vidaña I 2013 Phys. Rev. C **88** 055802
[48] Bombaci I and Logoteta D 2013 Mon Not R Astron Soc Lett **433** L79
[49] Shapiro S L and Teukolsky S A 1983 *Black Holes, White Dwarfs andNeutron Stars* (Wiley, New York, 1983).
[50] Baym G, Pethick C and Sutherland D 1971 Astrophys. J. **170** 299
[51] Negele J W and Vautherin D 1973 Nucl. Phys. A **207** 298
[52] Steiner A W, Lattimer J M and Brown E F 2010 Astrophys. J. **722** 33
[53] Steiner A W, Lattimer J M and Brown E F 2013 Astrophys. J Lett. **765** L5